JOURNAL OF Applied Polymer SCIENCE

Flame Retardant Polyurethane Nanocomposite: Study of Clay Dispersion and Its Synergistic Effect with Dolomite

Rafieh-Sadat Norouzian Amiri,[1,2] Teija Tirri,[1] Carl-Eric Wilen[1]

[1]Center of Excellence for Functional Materials (FUNMAT), Laboratory of Polymer Technology, Abo Akademi University, Biskopsgatan 8, FIN-20500 Abo, Finland

[2]Department of Chemistry, University of Mazandaran, Babolsar, Iran

Correspondence to: C.-E. Wilen (E-mail: cwilen@abo.fi)

ABSTRACT: Polyurethane–clay nanocomposite adhesives were prepared by different synthetic routes and their microstructures were determined by X-ray diffraction measurements and from transmission electron microscopy images. The preparation method of the polyurethane nanocomposite adhesives was systematically changed, that is, condensation either in the presence or absence of catalyst, concentration and type of nanoclay, premixing order of nanoclay (nanoclay was either premixed with the polyol or isocyanate part) and by using MDI surface treated nanoclays. Depending on the polymerization conditions cluster, intercalated, and exfoliated clay structures were obtained. The flame retardant properties of the manufactured nanocomposite adhesives and the synergistic effect of clay in combination with dolomite were investigated by cone calorimeter and UL 94 vertical burning tests. The results indicate that addition of nanoclay reduces burning time and the total heat evolved (THE) at flame out, and that the type of assembled clay structure (cluster, intercalated or exfoliated) had a significant effect on the flame retardant property. Nanocomposites with 3 wt % of clay loading gave the shortest burning time, the lowest THE and also UL 94 V-2 ratings were reached, although the flame retardancy in terms of heat release rate and time to ignition was not improved. © 2012 Wiley Periodicals, Inc. J. Appl. Polym. Sci. 000: 000–000, 2012

KEYWORDS: nanoparticles; nanowires and nanocrystals; polyurethanes; flame retardance; morphology

Received 31 July 2012; accepted 21 November 2012; published online
DOI: 10.1002/app.38863

INTRODUCTION

The field of polymer nanocomposites is continuously expanding due to the ability of nanofillers to enhance many physical and mechanical properties in comparison to the pristine polymer. Nanocomposites offer access to materials possessing adapted properties and functions suitable for a wide array of high technology applications from sensors, medical devices, rocket propellants to flame retarded, barrier, and scratch-resistant products for various industries. Based on the type of industry and application area, nanocomposite technology has been successfully applied to both thermoset polymers and thermoplastics. In recent years, different types of nanoparticle fillers including layered silicates and carbon nanotubes have been the subject of intensive research.

The clay-based nanocomposites are among the most examined due to the relatively low price of clay minerals, their availability, and unique characteristics including their plate-like morphology with a high aspect ratio. The macroscopic phase behavior of polymer–colloid mixtures has been the subject of many theoretical and experimental studies. The dispersion state of the nanoclay in the polymer matrix can be described by cluster, intercalated (distanced but yet parallel layers), or exfoliated (fully dispersed) structures. In each case, the polymer chains are differently arranged in the nanocomposite matrix and thus the composite properties are intimately linked to the macroscopic structure of the inorganic filler in the nanocomposite. In many cases, the most significant improvements in reinforcement and barrier properties have been found for exfoliated systems and therefore various ways to enhance the dispersibility have been the topic of great interest.[1–6]

Polymer compatibility with the surface of the clay platelets is crucial for obtaining sufficient dispersion of the nanoparticles in the polymer matrix. One widely explored route to gain better interaction between the clay–polymer interfaces is to modify the nanoparticle surface by treatment with surfactants such as ammonium or imidazolium cationics with long alkyl tails. For instance, Seo et al.[7] prepared polyurethane nanocomposites by utilizing silanol surface modified clays that reacted with NCO groups of polymeric 4,4′-diphenyl methane diisocyanate (MDI) whereby an exfoliated structure was obtained that exhibited

enhanced mechanical properties at a clay loading of 3 wt %. Camino and coworkers[8] have shown that in the case of modified nanodispersed clay in polyurethane formulations, improved flame retardant properties can be reached for both intercalated and exfoliated structures. The improvement in flammability was in both cases attributed to the formation of char during combustion which lowered the peak of heat release in cone calorimeter tests. In the UL 94 vertical burning tests, the dripping tendency was significantly suppressed or even eliminated. Irrespective of the elimination of fire-induced dripping, the overall ranking decreased from V-2 for the pure polyurethane sample to unclassified ranking for the PU/clay nanocomposites, as the flame eventually propagated to the top of the specimen. The authors concluded that the nanoclay requires the addition of a conventional flame retardant to reach the UL 94 V-0 classification.

Traditional flame retardants for polyurethane formulations are based on haloalkyl phosphate ester compounds, such as tris-(chloropropyl) phosphate, that significantly increase time to ignition (TTI) and reduce the peak of heat release. The synergistic effect of different flame retarders from conventional phosphate containing[9–11] to novel flame retarders[12] with clay has been the subject of vast studies. Driven by the demand of a sustainable society, life cycle analysis and a change toward voluntary restrictions of potentially hazardous chemicals in the 21st century, a number of research groups have started to develop halogen-free flame retardant systems. As a consequence of this, we wanted to explore the utility of combining nanoclay with calcium magnesium carbonate $CaMg(CO_3)_2$, a readily used commercial filler in polyurethane adhesives.[13]

This article describes a stepwise *in situ* polymerization procedure for the production of polyurethane nanocomposite adhesives as well as its structural characterization and flame retardant properties in comparison to the corresponding neat polyurethane adhesive. To gain better understanding on how manufacturing parameters affect the breakup of clay agglomerates and the dispersion of the plate layers in polyurethane adhesives, the concentration of nanoclay, premixing order of nanoclay, and the presence or absence of catalyst were systematically changed. In addition, we present our findings regarding the correlation of the clay dispersion state with flame retardant properties of the polyurethane clay nanocomposite. The flame retardant properties were examined by cone calorimeter and UL 94 vertical burning tests.

EXPERIMENTAL

Material

Oligomeric diphenyl methane diisocyanate (MDI, average NCO-functionality 2.7 and M_w 366 g/mol, Huntsman), Castor oil (OH-functionality 3, M_w 933 g/mol, Alberding Boley), $CaMg(CO_3)_2$ (dolomite, average particle size 13.9 μm, Imerys), zeolite powder moisture scavenger (Sigma-Aldrich), and dibutyltin dilaurate catalyst (Sigma-Aldrich) were received from noncommercial sources and used as received (additional details not available). Two types of organoclays were used, Cloisite® 30B, a montmorillonite modified with bis-(2-hydroxyethyl) methyl, tallow alkyl ammonium cations (cationic exchange capacity of 90meq/100g clay), was supplied by Southern Clay Products (Texas, USA), Nanomer® I.28E, a montmorillonite modified with 25–30 wt % trimethyl stearyl ammonium cations, was supplied by Aldrich.

Sample Preparation

Preparation of Polyurethane Nanocomposite. To obtain finely dispersed organoclays in the polyurethane matrix, two synthesis methods were investigated, that is, a castor oil-based method and an MDI-based method. In the castor oil-based method, the organoclays were premixed with the polyol and in the MDI-based method with the isocyanate part. We expected the dispersion of silicate layers to be different depending on the method of premixing. Castor oil could due to inherently similar structure to the surfactant exhibit better compatibility with the clay in comparison to MDI. Conversely, MDI has active NCO groups which can react with the free hydroxyl groups on the clay surface and, subsequently, improve coupling between nanoparticles and the matrix.

Three different organoclays, that is, (1) Cloisite 30B, (2) Nanomer I.28E, and (3) MDI surface treated Cloisite 30B were used. The amount of clay was varied between 1, 3, and 5 wt %. Certain samples were also prepared without catalyst to avoid recombination of the scattered clay due to external gallery forces caused by the rapid growth of the polymer chains. Organoclays, not conventional clays, were used as they are known to have enhanced compatibility with hydrophobic polymer chains.

The compositions and preparation method of the samples are summarized in Table I. The base polyurethane was synthesized in a manner that the isocyanate to polyol ratio was kept at 1.05 [mol NCO/ mol OH]. Thus, the reaction of MDI with the clay surface was not taken into account. The reasoning behind this is that the extent of reactions between MDI and OH-groups of the clay surface is unknown and therefore any correction of molar ratio would be arbitrary. The quantities of $CaMg(CO_3)_2$, moisture scavenger, and catalyst were 35 wt %, 2 wt % and 12 μL, respectively. To avoid undesired foaming of the polyurethane adhesive, zeolite powder was used as moisture scavenger to remove any traces of water from the system (i.e., the isocyanate groups would react with moisture to form carbon dioxide as a blowing agent). The reference sample was prepared by

Table I. Type of Nanoclay and the Synthesis Procedure of Polyurethane Nanocomposite Adhesive

Sample	Nanoclay	Clay added to	Catalyst
I-30B-(1-3-5)[a]	Cloisite 30B	Castor Oil	Yes
II-30B-(1-3-5)	Cloisite 30B	MDI	Yes
III-30B-(1-3-5)	Cloisite 30B	MDI	No
IV-30B-3	MDI-ST[b] Cloisite 30B	MDI	Yes
I-I.28E-(1-3-5)	Nanomer I.28E	Castor Oil	Yes
II-I.28E-(1-3-5)	Nanomer I.28E	MDI	Yes
III-I.28E-(1-3-5)	Nanomer I.28E	MDI	No

[a]Weight percent of clay based on total adhesive amount.
[b]MDI surface treated.

adding $CaMg(CO_3)_2$, moisture scavenger, and catalyst into the castor oil and a mechanical stirrer was used to homogenize the mixture. Then MDI was added by manual mixing.

In the castor oil-based synthesis method, organoclay (1, 3, or 5 wt % based on total amount) was added to the castor oil and then mixed with a mechanical stirrer to a homogeneous mixture. After the premixing, ultrasound was applied for 15 min to further assist the penetration of chains of castor oil between clay layers, then, $CaMg(CO_3)_2$, moisture scavenger, catalyst and finally MDI were added. The final mixture was stirred manually and poured into appropriate Teflon molds to cure for 24 h.

In the MDI-based synthesis method, organoclay was first added to the MDI and mixed with a mechanical stirrer for 10 min. Due to the small size of MDI, we expected its easy diffusion between clay layers, thus ultrasound was not applied. Then, the appropriate amount of castor oil and $CaMg(CO_3)_2$ was added to the homogenized mixture. Catalyst was added when necessary and then molded.

Preparation of MDI Surface Treated Clay-Polyurethane Nanocomposite

A published procedure for modifying organoclay with polymeric 4,4′-diphenyl methane diisocyanate was applied to prepare the polyurethane nanocomposite IV-30B-3 with the MDI surface treated organoclay.[7]

Cloisite 30B (3 wt % based on total amount) was added to the MDI and mixed at 2000 rpm with a mechanical stirrer in an oil bath for 2 h. The temperature of the oil bath was maintained at 50°C. After premixing, ultra sound was applied to the mixture for 15 min. Castor oil, $CaMg(CO_3)_2$, and catalyst were added to the modified clay, stirred, and poured into Teflon moulds and allowed to cure for 24 h.

Characterization

Dispersion. To determine the dispersion state of the clay layers in the polymer matrix, X-ray diffraction (XRD) measurement and transmission electron microscopy (TEM) were used. The XRD measurements were performed with Philips (Panalytical) X'Pert Pro MPD (Almelo, Netherlands). Monochromated CuKα radiation generated with acceleration voltage of 40 kV and cathode current of 50 mA was used. The primary X-ray beam was collimated using 0.25° axial divergence slit and a 15 mm equatorial mask. At the diffracted beam side 0.25° antiscatter slit and a 0.25 mm receiving slit were used before the proportional counter. The diffractograms of the samples were recorded from 1.5 to 11.5° with a scanning speed of 0.04° per 6 s. The measured diffractograms were analyzed using X'Pert HighScore 1.0 program.

TEM images were obtained on a JEM-1200EX and 1005X at an accelerating voltage of 60 kV. Ultrathin sections, approximately 60–100 nm thick, were cut from the embedded polyurethane nanocomposites in Epon™ epoxy resin using a diamond knife with ultramicrotome, placed on 300 mesh grids and examined by TEM.

Flammability

Flammability of polymers is assessed through ignitability, flame spread, and heat release. To cover all of the aforementioned aspects, cone calorimeter and UL 94 tests were chosen to measure the flame retardancy of the nanocomposites. The ignitability and heat release was measured by a cone calorimeter. The UL-94 test can give an overview of the flammability and flame spread.

Cone calorimetric measurements were done with the FTT cone calorimeter equipped with a Xentra gas analyzer. The samples were irradiated at 50 kW/m^2 and the exhaust gas flow was set to 24 L/s. Tests were performed according to ISO 5660-1 standard having the end test criterion at flame out.[14] Burning time is given as a difference between the ignition time and time of flame out. The samples were $10 \times 10 \times 0.3$ cm^3 in size and were prepared using Teflon molds. The average heat release rate (HRR_{ave}, kW/m^2) and its peak value (HRR_{peak}, kW/m^2), total heat evolved (THE) at flame out (MJ/m^2), and TTI (s) were directly given by the software.

For the UL 94, test samples were cut in $12 \times 1 \times 0.3$ cm^3 stripes and positioned vertically in the UL 94 chamber. Cotton was placed 30 cm below the specimen to monitor the dripping behavior. A Bunsen burner flame (height 20mm) was applied to the specimen twice (10 s each). Samples were classified as V-0, V-1, V-2, or no classification (NC) in accordance with the UL 94 vertical burning test standard.[15]

RESULTS AND DISCUSSION

Clay Dispersion

The structural analysis of the nanocomposite may help to establish a correlation between polymerization parameters and the derived morphological states of polyurethane–nanoclay nanocomposites. Furthermore, the structural analysis is also vital for a better understanding of the structure-property relationship of the nanocomposite system containing different intergallery spacing of nanoclay. Therefore, we wanted to characterize the obtained nanocomposite morphologies in detail by means of XRD and TEM analyses. The XRD patterns of the nanocomposite samples are depicted in Figures 1 and 2.

Figure 1(a) shows the XRD pattern of the 30B-3 nanocomposite samples with different preparation methods. The neat Cloisite 30B exhibits a diffraction peak at $2\theta = 4.6$ as shown in Figure 1(a) giving a d spacing of 19.25Å, whereas for the nanocomposite sample I-30B-3, a peak at 4.5 was clearly observed. Thus, the recorded diffraction peaks are very close to each other. This result indicates that the nanocomposite denoted I-30B-3 has a cluster type of morphology with no distinct changes in the gallery height proved by its TEM image [Fig. 1(b)]. In Figure 1(a), the graph for II-30B-3 shows only a small and broad peak in the 2θ at 2, this peak has been shifted by 2.6 degrees to the left from the base nanoclay diffraction, which indicates that some polyurethane molecular chains have been intercalated between the nanoclay galleries and the d spacing has increased from 19.25 to 45.29 Å. The intercalated morphology is shown in Figure 1(c). Finally, for III-30B-3, no specific peak could be observed in the XRD graph. This indicates that the nanoclay plates have been completely exfoliated when the synthesis of nanocomposite has been performed under slow polymerization conditions in the absence of catalyst [Figure 1(d)].

Applied Polymer SCIENCE

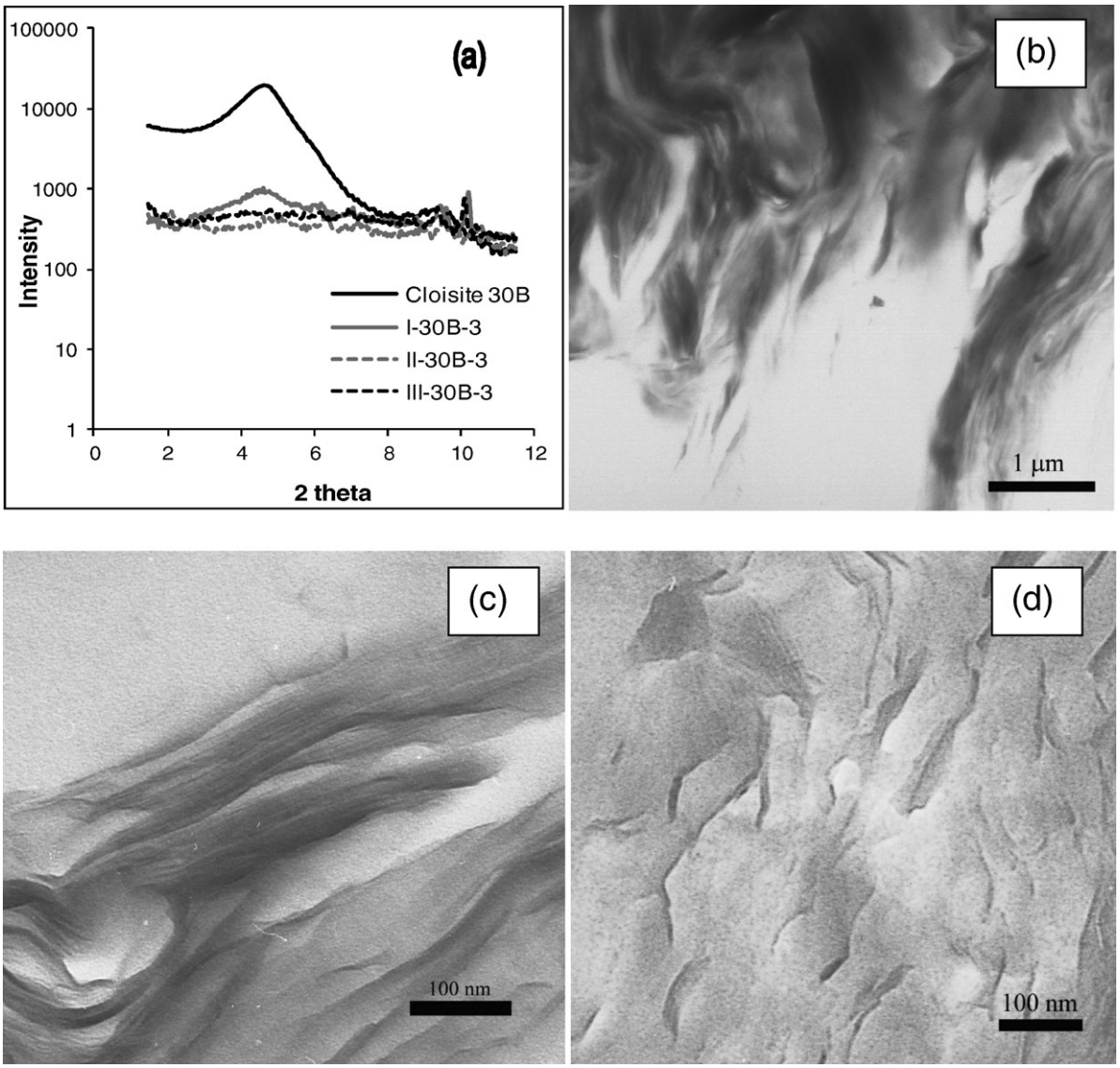

Figure 1. Morphological analysis of Cloisite 30B based polyurethane nanocomposite. (a) XRD graphs of the nanocomposite and TEM images of (b) I-30B-3, (c) II-30B-3, and (d) III-30B-3.

The XRD pattern and TEM image of the MDI surface treated nanocomposite was also studied. As observed in Figure 2(a), this pattern gives a very smooth line particularly in the 2θ area of the Cloisite 30B crystal peak, thereby providing evidence of the formation of a uniform dispersion and an exfoliated structure. Nanometer thin clay layers are scattered in the polyurethane matrix, as observed in the TEM image [Figure 2(b)].

The XRD patterns of the nanocomposites with Nanomer I.28E are shown in Figure 3(a). In the case of pure Nanomer I.28E, a strong peak at 3.7 was clearly observed indicating a d spacing equal to 23.83 Å, whereas for the I-I.28E nanocomposite a weak peak in the 2θ of 2.5 and a much smaller one at 4.7 were recorded, respectively, showing a 35 and 18.78 Å d spacing and no characteristic peak of nanomer at 3.7 could be observed. Thus, we contribute the shift of the peak from 3.7 to 2.5 to indicate an intercalated structure of the nanocomposite I-I.28E. The smaller peak at 4.7 can be a sign of recombination of the clay layers forming a more compact cluster due to the force caused by polymerization of chains in the matrix. For the II-I.28E and III-I.28E-3 samples, no peaks can be detected which implies the achievement of exfoliated morphologies. The TEM image of the exfoliated morphology of sample II-I.28E is shown, as an example, in Figure 3(b).

From the foregoing, it is clear that the preparation method and reaction conditions in the stepwise route to nanocomposites synthesis determine to a large extent the type of polyurethane–clay microstructure, that is, cluster, intercalated or exfoliated structure. This type of study not only helps us to understand the ongoing interaction and reactions between the organoclay and polyurethane but also gives us the opportunity to study its impact on other properties of the nanocomposites with these diverse structures such as flame retardancy.

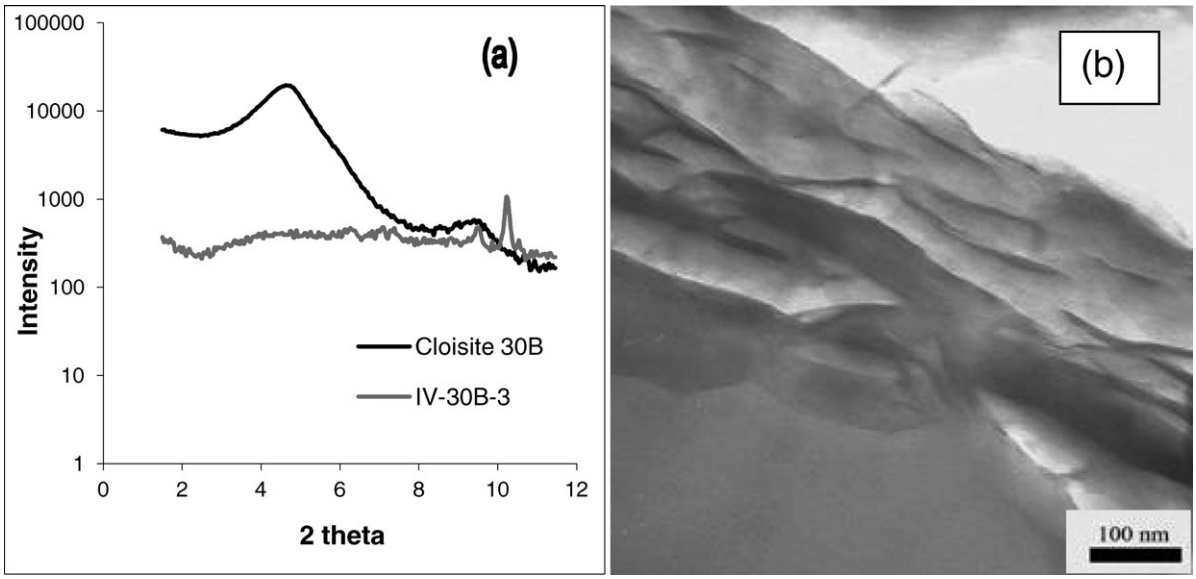

Figure 2. XRD graph and TEM image of the MDI surface treated 30B based polyurethane nanocomposite (IV-30B-3).

The clay dispersion in the I-30B-3 nanocomposite was identified as cluster morphology. This means that the compatibility between the castor oil and the surfactants on the clay surface was not powerful enough to let the castor oil chains penetrate in to the clay galleries. Thus, phase separation of the clay and polymer[16] results in the polymerization of the polyurethane around the stacks of Cloisite 30B and thereby to the formation of cluster morphology.

The intercalated morphology of the II-30B-3 indicates that an effective reaction between the MDI and the nanoclay was present which results in a larger gallery distance in the final nanocomposite. So, here some polyurethane chains were formed in the clay galleries but, the clays were still not fully dispersed.

A key parameter that can have a negative impact on the polymer dispersion is the force exerted by the extra gallery polymer network. Because polymerization takes place at an increased rate, as in our case when catalyst was added, the pressure implied by the fast-growing polymers on the nanoclay can cause the clay layers to recombine into agglomerates. Thus, too rapid polymerization rate may alter a potentially exfoliated nanocomposite to a cluster or an intercalated one. In contrast, if polymerization is carried out slower the polymer chains have enough time to develop around the dispersed clay plates.[17] Based on this reasoning, polymerization was repeated using the same condition as previously for II-30B but without catalyst. Thus, adequate time was given for the formation of the nanocomposite in III-30B-3. The XRD patterns reveal an exfoliated

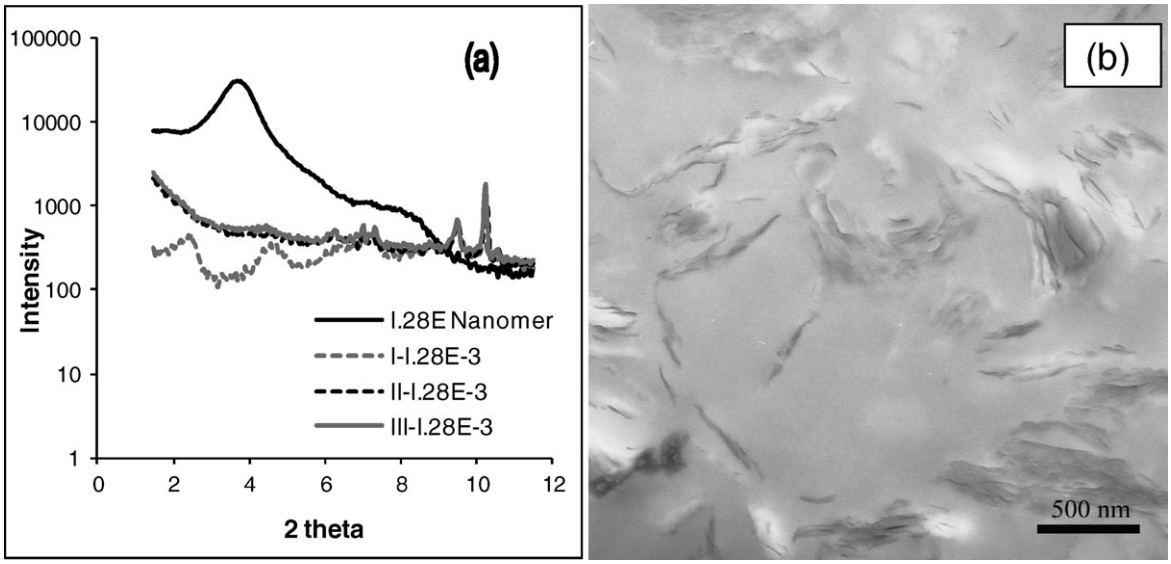

Figure 3. (a) XRD graph of the I.28E Nanomer based polyurethane nanocomposites and (b) the TEM image of II-I.28E-3.

Table II. Cone Calorimeter Data for the 30B Nanocomposites

Sample	Reference	I-30B (Cluster)[a]			II-30B (Intercalated)[a]			III-30B (Exfoliated)[a]		
Wt % nanoclay	0	1	3	5	1	3	5	1	3	5
Burning time[s]	505	332	216	270	312	246	368	304	240	453
HRR_{peak} [kW/m^2]	389	439	506	415	407	381	373	348	404	374
HRR_{ave} [kW/m^2]	152	202	297	248	235	247	233	204	273	174
THE [MJ/m^2]	77	66	64	66	72	60	85	61	65	78
TTI [s]	40	36	34	35	37	39	37	36	30	37

[a]Structure analyzed for samples containing 3 wt % of clay.

structure for this nanocomposite, so the dispersed clay remained apart until the formation of the nanocomposite was completed. Consequently, polymerization rate has also an influence on the clay dispersion in the polymer matrix.

The effect of clay modification on the dispersion mode was also studied. The exfoliated structure for IV-30B-3 shows that when MDI surface treated Cloisite 30B is used, a more effective reaction takes place resulting in a uniform dispersion of clay even in the presence of a catalyst. Thus, by using this preparation method, an exfoliated structure can be achieved when the curing reaction is speeded up by the catalyst.

The results indicate that Nanomer I.28E clay has a better affinity with the castor oil compared to Closite 30B because of its higher organophilic nature. As predicted, the better compatibility between castor oil and Nanomer I.28E resulted in an intercalated structure in the I-I.28E-3 nanocomposite compared to the cluster in I-30B-3. Another aspect that can affect the different dispersion states in the two nanoclays can be the gallery height. The $d_{001}$of Cloisite 30B is measured to be 19.25 Å with Bragg's law and for Nanomer I.28E the d_{001} is 23.83Å. A bigger gallery distance results in an easier inlet of the castor oil before polymerization because of a smaller friction[18,19] and after polymerization in the gallery spacing it gives an intercalated structure. An exfoliated structure is observed for the II-I.28E-3 and III-I-28E-3 nanocomposites in which smaller MDI could easily penetrate into the galleries.[20] In addition, both nanocomposites produced delaminated clays. The omission of catalyst had no distinct effect.

Flammability

Cone Calorimeter

Depending on the application of the polyurethane, a specific flammability test needs to be carried out and different flammability requirements need to be met before acceptance for their industrial utilization. The cone calorimeter test is a very useful bench-scale test developed for standardization purposes and it can simultaneously allow a prediction of large-scale fire behavior.[17]

Many commercial polyurethane formulations contain fillers such as calcite ($CaCO_3$) or dolomite ($CaMg(CO_3)_2$) as they, among other benefits, decrease flammability.[13,21] However, the shortcomings are that rather high loadings of 30–70 wt % of the fillers are needed and normally their performance needs to be enhanced by a synergist. As a reference, we wanted to investigate the flammability of polyurethane containing 35% $CaMg(CO_3)_2$ without any nanoclay by cone calorimeter and compare it with samples containing dispersed clay in various concentrations and microstructures. Table II shows the burning time, peak of HRR (HRR_{peak}), average HRR (HRR_{ave}), THE at flame out, and TTI of the samples containing 1, 3, and 5 wt % of 30B nanocomposite versus polyurethane prepared without the nanoclay as a reference.

The data in Table II clearly show the difference in fire behavior of polyurethane in the presence of nanoclay. As observed, addition of clay significantly reduces the burning time. The nanocomposites with 3 wt % of clay loading gave the shortest burning times. Conversely, the maximum amount of HRR (HRR_{peak}) and the average HRR (HRR_{ave}) increased. The nanoclay addition seems to momentarily increase intensity of burning which is translated into a sharp HRR peak on the HRR curve. In contrast, Berta et al.[8] showed in their studies of the effect of organoclay 30B on the HRR of polyurethane that the average HRR and its peak were reduced compared to the pristine polyurethane sample, and they obtained the best results when using a 3 wt % loading of clay. The differences between

Table III. Cone Calorimeter Data for the I.28E Nanocomposites

Sample	Reference	I-I.28E-3 (Intercalated)[a]	II-I28E-3 (Exfoliated)[a]	III-I.28E-3 (Exfoliated)[a]	IV-30B-3 (Exfoliated)[a]
Burning time[s]	505	229	206	233	325
HRR_{peak} [kW/m^2]	389	436	444	456	435
HRR_{ave} [kW/m^2]	152	267	295	299	233
THE [MJ/m^2]	77	60	60	69	75
TTI [s]	40	31	34	37	45

[a]Structure analyzed for samples containing 3 wt %.

Table IV. UL 94 Data for the 30B Nanocomposites

Sample	Reference	I-30B (Cluster)[a]			II-30B (Intercalated)[a]			III-30B (Exfoliated)[a]		
Percent		1	3	5	1	3	5	1	3	5
Classification	NC[b]	V-2	V-2	NC	V-2	V-2	NC	NC	V-2	NC
Average burning time	-	11.28	27.2	-	11.3	39.8	-	-	19.83	-
Burning style	-	Fast	Slow	Slow	Fast	Slow	Slow	Vigorous	Fast	Vigorous

[a]Structure analyzed for samples containing 3 wt % of clay.
[b]Nonclassified

the HRR behaviors can be attributed to the presence of dolomite in our samples.

To get more details on the burning behavior of nanocomposites, the THE at flame out and TTI were recorded. The THE values in Table II show an overall decrease in comparison with the reference polyurethane, and again somewhat better results were obtained with the clay loading of 3 wt %. There was a decrease in the detected TTI of the clay bearing samples compared to the polyurethane reference. This result may be assigned to a partial thermal degradation of surfactants in the organoclay at the early stages of burning.[22,23]

The results obtained for the polyurethane nanocomposite prepared from the MDI surface treated Cloisite 30B (IV-30B-3) are presented in Table III. The results show a similar trend compared to the delaminated 30B nanocomposites, no enhanced effect were revealed by this modification in terms of flammability.

Due to the promising performance of Cloisite 30B clays at the loading of 3 wt %, we decided to study Nanomer I.28E further at this loading. The cone calorimeter data presented in Table III show the same tendency which was seen also for the 30B nanocomposite. The TTI and burning times decreased, whereas increase in the HRR_{ave} and HRR_{peak} was observed in comparison to the reference sample. The THEs for these samples decreased compared to the reference polyurethane alike the 30B nanocomposites.

Based on the cone calorimeter data, no straight forward conclusion can be made regarding the effect of clay dispersion state. However, it is evident that the addition of clay has some positive effect on the THE at the flame out, but the HRR and HRR_{peak} results did not show such improvements in fire retardancy.

UL-94 Flame Retardant Tests

The UL 94 test was applied to assess ignitability and flame spread of polymeric materials exposed to a small flame. Table IV shows the classification of the 30B nanocomposites compared to the reference sample containing only dolomite. To compare the effect of clay loadings and assess the consequence of dispersion states, some important features in the flame spread, that is, average burning time and burning style, were also noted.

One can see from the comparison of the reference sample and the nanocomposite that V-2 classification could not be reached without the use of clay. For both I-30B samples with 1 and 3 wt % of clay loadings, a V-2 classification was reached, but the samples at 3 wt % loading burned slower with a smaller flame. So with an increase of clay loading up to 3 wt %, the clay plates were acting as a heat barrier controlling the flame spread and resulting in a mild flame, but as the loading increased to 5 wt % the flame burned slowly but without self-extinguishing and therefore a nonclassified ranking was obtained.

The same pattern is observed for the II-30B samples. In the III-30B samples, the 3% loading was the best one due to its V-2 classification and slower burning. Comparing the 30B nanocomposite samples, with different clay dispersion morphology, it can be seen that as the clay delaminates and starts to intercalate and further exfoliate, from sample I to II and further III, the flame spread assessed by the burning time and burning style increases. The slowest flame spread was observed for the cluster nanocomposite regarding the burning time, burning style, and also the best classification. The burning time increased for the intercalated structure, but when an exfoliated structure was formed the samples burned to the end (except at 3 wt % loading) leading to a nonclassified ranking. This result can be assigned to the ease of burning of the surfactants on the clay surface.[24] As the clays form an exfoliated structure, more surfactant is exposed to the flame leading to a faster flame spread. This in turn causes an overlapping effect on the flame retardancy of the raw clay. Table V shows the behavior of the exfoliated I.28E nanocomposites in terms of flame spread.

In this case, V-2 classification was only observed for the samples having 1 wt % loading of the nanoclay. The exfoliation of clays

Table V. UL 94 Data for the I.28E Nanocomposites

Sample	II-I.28E			III-I.28E		
Percent	1	3	5	1	3	5
Classification	V-2	NC	NC	V-2	NC	NC
Average burning time	6.77	-	-	28.95	-	-
Burning style	Very low	Vigorous	Vigorous	Fast	Vigorous	Vigorous

results in the ready exposure of surfactants to the flame zone and therefore the high modified clay loadings lead to a vigorous burning behavior. Whereas, at low loadings of 1 wt % clay, the burning effect of surfactant is still seemingly smaller than the retarding effect of clay. From this, we can conclude that organoclays have two different effects, on one hand they help the exfoliation and thereby suppression of fire and on the other hand they negatively contribute to flammability by increasing the fuel load. We envision that the best results would potentially be obtained by utilizing an organoclay having surfactants with flame retardant properties in combination with the high exfoliation ability.

CONCLUSIONS

The present results reveal that by fine-tuning the preparation method, reaction conditions, and type of nanoclay in the stepwise synthetic route to polyurethane–clay nanocomposite adhesives, one can control the type of microstructure. Thus, by carefully altering the key reaction parameters one can prepare nanocomposites having either cluster, intercalated or fully exfoliated structures and thereby enabling the assessment of microstructure-flame retardant property relationships. We have demonstrated that the flame retardant properties in the polyurethane clay nanocomposite depend on the concentration and state of dispersion of organoclay in the polyurethane matrix. According to the cone calorimeter results, nanoclay exhibited a weak FR effect with the conventional flame retarding $CaMg(CO_3)_2$ filler, that is, a decrease in THE was observed for the adhesive samples containing nanoclay. In contrast, the HRR and HRR_{peak} values, which are the most important criteria in terms of fire behavior, did in fact slightly increase in the presence of nanoclay. Whereas again, the UL-94 test showed some positive effect of nanoclay with dolomite and at an optimal loading of 3 wt % of nanoclay a polyurethane–clay nanocomposite adhesive formulation was formed that passed the UL94 V-2 rating. In addition, this study showed the dual and contradictive role of using surface modified nanoclays. Thus, the surfactants promote the formation of an exfoliated structure, and in this sense it reduces the flammability. Whereas, on the other hand, surfactants promote fast flame spread, especially at high clay loadings with exfoliated morphology by increasing the total fuel load in the composite. The relatively exposed surfactants in the exfoliated structure have a tendency to burn vigorously due to decomposition of the surfactant (Hofmann elimination reaction). As a consequence of this, when applying modified clay in a flame-resistant product, the burning effect of the surfactant should be taken into account in order not to lose the positive effects obtained by an exfoliated structure.

REFERENCES

1. Maji, P. K.; Guchhait, P. K.; Bhowmick, A. K. *J Mater. Sci.* **2009**, *44*, 5861.
2. Wan, S.; Hu, Y.; Li, Z.; Wang, Z.; Zhuang, Y.; Chen, Z.; Fan; W. *Colloid Polym. Sci.* **2003**, *281*, 951.
3. Gilman, J. W.; Jackson, C. L.; Morgan, A. B.; Harris, R. Jr., Manias, E.; Giannelis, E. P.; Wuthenow, M.; Hilton, D.; Phillips, S. H. *Chem. Mater.* **2000**, *12*, 1866.
4. Berta, M.; Saiani, A.; Lindsay, C.; Gunaratne, R. *J. Appl Polym. Sci.* **2009**, *112*, 2847.
5. Seo, W. J.; Sung, Y. T.; Kim, S. B.; Lee, Y. B.; Choe, K. H.; Choe, S. H.; Sung, J. Y.; Kim W. N. *J. Appl. Polym. Sci.* **2006**, *102*, 3764.
6. Chung, Y-C.; Cho, T. K.; Chun, B. C. *Fibers Polym.* **2008**, *9*, 7.
7. Seo W. J.; Sung Y. T.; Han S. J.; Kim Y. H.; Ryu O. H.; Lee H. S.; Kim W. N. *J. Appl. Polym. Sci.* **2006**, *101*, 2879.
8. Berta M.; Lindsay C.; Pans G.; Camino G. *Polym. Degrad. Stab.* **2006**, *91*, 1179.
9. Isitman, N. A.; Kaynak, C. *Polym. Degrad. Stab.* **2010**, *95*, 1523.
10. Modesti, M.; Lorenzetti, A.; Besco, S.; Hrelja, D.; Semenzato, S.; Bertani, R.; Michelin, R.-A. *Polym. Degrad. Stab.* **2008**, *93* 2166.
11. Song, L.; Hu, Y.; Tang, Y.; Zhang, R.; Chen, Z.; Fan, W. *Polym. Degrad. Stab.* **2005**, *87*, 111.
12. Tai, Q.; Yuen, R. K. K.; Song, L.; Hu, Y. *Chem. Eng. J.* **2012**, *183*, 542.
13. Tirri, T.; Aubert, M.; Wilén, C.-E.; Pfaendner, R.; Hoppe, H. *Polym. Degrad. Stab.* **2012**, *97*, 375.
14. ISO 5660–1. Heat Release Rates from Building Products (Cone calorimeter Method); The International Organization for Standardization: Geneva; **1993**.
15. UL 94 Standard for Tests for Flammability of Plastic Materials for Parts in Devices and Appliances; Underwriters Laboratories Inc.: Northbrook, **1998**.
16. Ginzburg V. V.; Singh C.; Balazs, A. C. *Macromolecules* **2000**, *33*, 1089.
17. Flame Retardant Polymer Nanocomposites; Morgan, A. B., Wilkie, C. A., Eds.; Wiley: Hoboken, **2007**.
18. Manias, E.; Chen H.; Krishnamoorti R.; Genzer J.; Kramer E. J.; Giannelis E. P. *Macromolecules*, **2000**, *33*, 7955.
19. Lan T.; Pinnavaia T. J. *Chem. Mater.* **1994**, *6*, 2216.
20. Taheri Q. N.; Norouzian A. R. *J. Polym. Eng.* **2010**, *30*, 461.
21. Lindholm J, Brink A, Wilén C-E, Hupa M. *J. Appl. Polym. Sci.* **2012**, *123*, 1793.
22. Li Z-F.; Wang, S-J.; Li, J-Y. *Front. Mater. Sci. China.* **2008**, *2*, 271.
23. Bourbigot, S.; Devaux, E.; Flambard, X. *Polym. Degrad. Stab.* **2002**, *75*, 397.
24. Norouzian, A. R.; Taheri, Q. N.; Sharifi, S. N. *J. Macromol. Sci Part B: Phys.* **2009**, *48*, 955.